

Li deficiencies in LiNbO₃ films prepared by pulsed laser deposition in a buffer gas

J. Gonzalo,^{a)} C. N. Afonso,^{b)} and J. M. Ballesteros
Instituto de Optica, CSIC, Serrano 121, 28006 Madrid, Spain

A. Grosman and C. Ortega

*Groupe de Physique des Solides, Universités de Paris VII et VI, URA 17 du CNRS, 2 Place Jussieu,
75251 Paris Cedex 05, France*

(Received 1 April 1997; accepted for publication 18 June 1997)

The origin of Li deficiency in films grown by laser ablation of single-crystal LiNbO₃ targets in a buffer gas has been investigated by analyzing the stoichiometry of the deposited films as a function of the following parameters: the distance target-substrate, the nature of the buffer gas (He, O₂, and Ar) and the deposition configuration. The results show that significant Li losses are related to scattering processes during the expansion regime which are higher the higher the mass of the gas species. The results show that the Li content of the films can be enhanced by setting the substrate either at distances larger than the plume length or in a configuration in which the substrate is not facing the target. © 1997 American Institute of Physics. [S0021-8979(97)06418-9]

I. INTRODUCTION

Lithium niobate (LiNbO₃) is known to have excellent nonlinear properties, including piezo-electric, acousto-optic, and electro-optic properties.¹ These properties make LiNbO₃ a promising candidate for many opto-electronic applications such as modulators, frequency converters, or storage media^{2,3} if the production of high quality films on substrates with lower refractive index can be achieved.

Several deposition methods have been attempted to grow high quality LiNbO₃ films, including molecular beam epitaxy,⁴ liquid phase epitaxy,⁵ sol-gel process,⁶ rf sputtering,⁷ and more recently, pulsed laser deposition (PLD).⁸⁻¹² The latter technique has been very successful in the growth of high T_c superconducting films and other complex oxides.^{13,14} The main limitation when producing LiNbO₃ films by PLD is the loss of Li in the films, which promotes the growth of a Li deficient phase, such as LiNb₃O₈.^{8,10,12} The use of Li-enriched sintered targets^{10,11} or mixed O₂/Ar gas ambients⁸ can partially overcome this problem and lead to stoichiometric LiNbO₃ films; nevertheless, the conditions for producing high quality films are still unclear, and in the literature some controversial results can be found. Some authors⁸ claim that no single phase films can be obtained by ablation of stoichiometric LiNbO₃ in a pure oxygen environment, whereas others succeeded.¹² In other cases,^{10,11} no stoichiometric films were obtained by ablation of stoichiometric targets, this result being attributed to the re-evaporation of the adsorbed Li on the film surface upon rising the temperature.¹⁰ In addition, the use of single-crystalline stoichiometric targets to grow stoichiometric films might be desirable, because their use has been reported to lead to the growth of particulate-free films.⁹ Therefore, further studies of the influence of the deposition parameters

on the PLD process have to be performed in order to elucidate these points.

In an earlier work, we combined Rutherford backscattering spectrometer (RBS) and nuclear reaction analysis (NRA) to study the influence of the target composition, the laser fluence and the oxygen pressure applied during deposition on the stoichiometry of films grown by ablation of LiNbO₃.¹¹ The results showed that a Li/Nb molar fraction of 1.5–2.0 was required to obtain nearly stoichiometric films in agreement with other reports,¹⁰ and this result depended very little on both laser fluence and oxygen pressure. The aim of this work is to investigate the influence of the target-substrate distance, the nature of the buffer gas and the substrate configuration, on the stoichiometry of films grown by ablation of single-crystalline targets. The results are analyzed in terms of the expansion dynamics of the plasma and the role of collisional processes leading to a preferential scattering of the lighter species.

II. EXPERIMENT

A LiNbO₃ single-crystal ([Li]/[Nb]=0.94 in the melt) has been ablated using an ArF excimer laser ($\lambda=193$ nm, $\tau=12$ ns FWHM) focused on the target surface. The target was mounted in a rotating holder and placed in a vacuum chamber evacuated to a residual pressure of 2.0×10^{-7} mbar, which will be referred to hereafter as vacuum. The angle of incidence of the laser beam was 45°, and the laser energy density at the target surface was ≈ 2 J/cm². The films were grown on Si(100) substrates held at room temperature by ablating the target during 60 minutes after 5 minutes of pre-ablation, both at 5 Hz. Although the target composition might be modified by the laser ablation process¹⁵ and thus lead to non-stoichiometric films, this cleaning procedure together with the long deposition time guarantees that a steady state in the target composition is reached and therefore all the films are deposited under similar target conditions.

The influence of the target-substrate distance (d) on the composition of the films has been analyzed by growing films

^{a)}Present address: Department of Applied Physics, University of Hull, Hull, HU6 7RX, United Kingdom.

^{b)}Electronic mail: cnafonso@pinar1.csic.es

on substrates located at $d=20, 33$, and 40 mm from the target in 7.0×10^{-2} mbar of oxygen. The role of the buffer gas was studied by growing films at a fixed distance ($d=33$ mm) in four different environments: vacuum and 7.0×10^{-2} mbar of He, O₂, and Ar. Finally, since the scattering of the ejected species by the gas atoms and/or molecules is known to play a crucial role on the stoichiometry of the films grown by PLD^{16–18} an experiment involving simultaneous deposition on two substrates was performed. The substrates were located at two sites as described in detail elsewhere.¹⁸ One was along the target normal (S1) at a fixed distance ($d=33$ mm) and facing the target, and the second one (S2) was shifted upwards and located such as the deposit was non-facing the target. Two different configurations were considered for substrate S2 during the deposition process: (i) the re-emission (S2RE) configuration, in which both S1 and S2 substrates were present and (ii) the gas scattering (S2GS) configuration in which only the S2 substrate was present, and therefore, the material deposited could only come from the scattering of the ablated species by the buffer gas.

The composition of the films was determined at their thicker region by simultaneous RBS and NRA using a deuteron beam at 0.85 MeV.¹¹ The Nb content was detected by RBS, while the Li and the O contents were determined by NRA through the ${}^6\text{Li}(d, \alpha_0){}^4\text{He}$ and ${}^{16}\text{O}(d, p){}^{17}\text{O}^*$ reactions, respectively. We have considered as representative ratios to describe the composition of the films, the lithium and oxygen to niobium atomic ratios ($N_{\text{Li}}/N_{\text{Nb}}$ & $N_{\text{O}}/N_{\text{Nb}}$). The absolute values of the film composition have been determined by comparison with references known within 3% (O and Nb) and 20% (Li). The reduced precision of the Li reference leads, therefore, to a low precision in the determination of the absolute values. Nevertheless, the changes of relative composition of films grown in the different experimental conditions remain unaffected by this imprecision and are only affected by the statistical errors (root-mean-square errors) that are in all cases in the range 4–7.5%. Further details of the experimental configuration used for analysis and the determination of the experimental errors can be found elsewhere.¹¹

III. RESULTS

Figure 1(a) shows the total amount of atoms ($N_{\text{tot}} = N_{\text{Li}} + N_{\text{Nb}} + N_{\text{O}}$) measured in films deposited on the facing substrate (S1) at different distances from the target in 7.0×10^{-2} mbar of O₂. It is seen that the amount of material deposited on the substrate decreases when the distance from the target increases, this decrease being sharper for $d > 33$ mm. Figure 1(b) shows the dependence of the $N_{\text{Li}}/N_{\text{Nb}}$ and $N_{\text{O}}/N_{\text{Nb}}$ ratios measured in the same films. Both ratios decrease as d is increased to 33 mm; nevertheless, they increase for greater distances. Figure 1(b) also shows that the films are in all cases deficient in Li, with $N_{\text{Li}}/N_{\text{Nb}}$ ratios well below the desired value for LiNbO₃ ($N_{\text{Li}}/N_{\text{Nb}} = 1$). Finally, both Figs. 1(a) and 1(b) clearly show that there is a change in behavior near $d=33$ mm.

The presence of a buffer gas has also a strong influence on the relative composition of the films as it can be seen in Fig. 2 for films grown at $d=33$ mm in different gas environ-

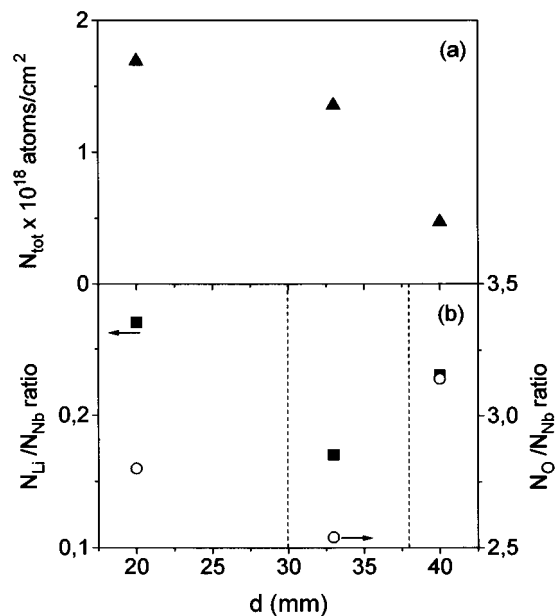


FIG. 1. (a) Total amount of atoms (N_{tot}), and (b) Li and O to Nb atomic ratios ($N_{\text{Li}}/N_{\text{Nb}}$, $N_{\text{O}}/N_{\text{Nb}}$) of films deposited on substrate S1 at different distances ($d=20$ mm, 33 mm and 40 mm) from the target surface in 7.0×10^{-2} mbar of O₂. The dashed lines correspond to the estimation of the plume length according to the adiabatic expansion model.

ments: vacuum and 7.0×10^{-2} mbar of He, O₂, or Ar. It is clearly seen that, although the $N_{\text{Li}}/N_{\text{Nb}}$ and $N_{\text{O}}/N_{\text{Nb}}$ ratios are always below the stoichiometric content, they generally follow opposite trends: $N_{\text{Li}}/N_{\text{Nb}}$ decreases and $N_{\text{O}}/N_{\text{Nb}}$ increases as the mass and radius of the gas species are increased.

The total amount of atoms (N_{tot}) (Fig. 3) and the relative composition of the films (Fig. 4) also have a strong dependence on the substrate configuration. Results obtained for films grown on the facing (S1) and non-facing (S2) substrates either in vacuum or in a buffer gas (He, O₂ and Ar) are included in both figures. It is clearly seen in Fig. 3 that the value of N_{tot} for films grown on the S1 and S2 substrates follow opposite trends: the former decreases and the latter increases as the mass and radius of the buffer gas increases.

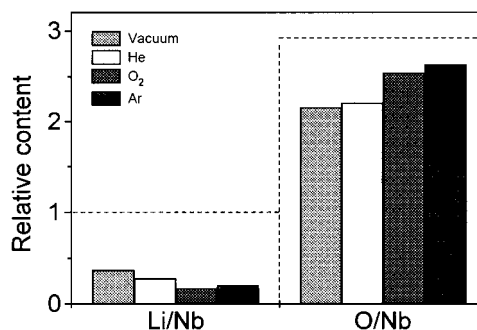


FIG. 2. Li and O to Nb atomic ratios ($N_{\text{Li}}/N_{\text{Nb}}$, $N_{\text{O}}/N_{\text{Nb}}$) for films deposited on substrate S1 at $d=33$ mm from the target surface in the different gas environments considered in this work (vacuum and 7.0×10^{-2} mbar of He, O₂, or Ar). The dashed lines indicate the composition of the target.

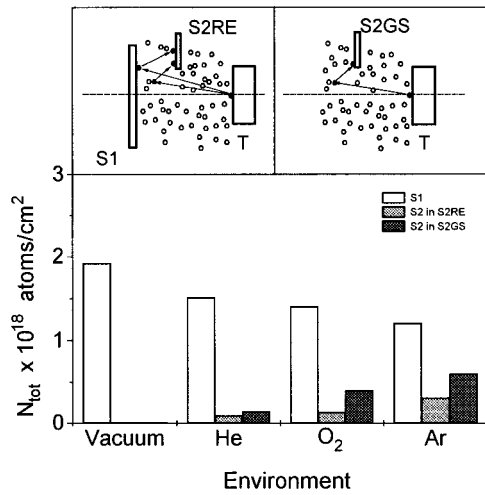


FIG. 3. Total amount of atoms (N_{tot}) for films deposited on substrates S1 and S2 in the two configurations considered (S2RE & S2GS) at a distance $d=33$ mm from the target surface in the different gas environments considered in this work (vacuum and 7.0×10^{-2} mbar of He, O₂, or Ar). The figure also shows the experimental configurations considered in this work: Re-emission (S2RE) and gas scattering (S2GS) configurations.

In vacuum, the amount of deposited material on S2 substrates is below our experimental resolution either in S2GS or S2RE configuration; whereas in the other buffer gases considered, the amount of deposited material in the S2GS

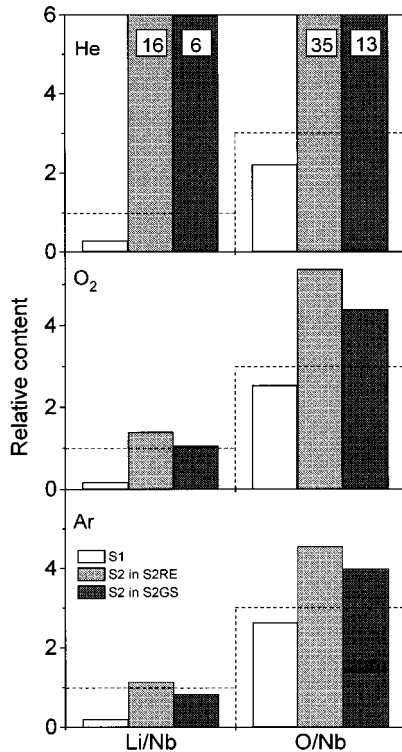


FIG. 4. Li and O to Nb atomic ratios ($N_{\text{Li}}/N_{\text{Nb}}$, $N_{\text{O}}/N_{\text{Nb}}$) for films deposited in 7.0×10^{-2} mbar of He, O₂, and Ar respectively on substrates S1 and S2 in the two configurations considered (S2RE & S2GS) at $d=33$ mm from the target surface. The dashed lines indicate the composition of the target.

configuration is higher than in the S2RE, similarly to what has been earlier reported for BiSrCaCuO films.¹⁸

Figure 4 shows the $N_{\text{Li}}/N_{\text{Nb}}$ and $N_{\text{O}}/N_{\text{Nb}}$ ratios for films grown in the different configurations and buffer gases considered. Both ratios are always higher for films grown on S2 substrates than for the corresponding films deposited on the S1 substrates. Films deposited on S2 substrates in the presence of a buffer gas shown a $N_{\text{Li}}/N_{\text{Nb}}$ ratio close to the stoichiometric value, or even much higher when using the lightest gas (He). The oxygen relative content ($N_{\text{O}}/N_{\text{Nb}}$) of films grown on S2 substrates is in all cases above the stoichiometric value, although the exact value depends on the particular buffer gas, and similarly to the $N_{\text{Li}}/N_{\text{Nb}}$ ratio, it decreases for films grown in heavier buffer gases (i.e., O₂ or Ar).

IV. DISCUSSION

The expansion of the plasma produced by laser ablation in the presence of a buffer gas is known to be dominated by the interaction of the ejected species and the background gas atoms or molecules.^{16,17,19–22} In the pressure range considered ($P < 0.1$ mbar), this interaction has been modeled^{16,17} in terms of the scattering of the ejected species by the buffer gas atoms and/or molecules, which alter the kinetic energy of the ejected species and eventually lead to changes in their angular distribution and in the composition of the grown films. The changes depend not only on the nature and pressure of the buffer gas, but also on the target-substrate distance.²² During the initial expansion, which extends along as a few mm from the target surface, the driver mass (ablation products) is very large compared with the mass of the driven gas; and thus, the buffer gas is pushed on by the leading edge of the plume, the plume expansion remaining unaffected by the presence of the buffer gas.^{19–21}

For higher distances, and once the ejected species interact with the buffer gas atoms and/or molecules, the decrease of the thickness and the compositional changes observed in Fig. 1 as a function of the target-substrate distance should be understood in terms of the collision probability and the angular dispersion. Assuming a simple model based on hard spheres²³ and taking into account that the mean velocity of the ablated species is much higher than the thermal mean velocity of the buffer gas species, the mean free path λ_1 of species 1 in buffer gas 2 is given by

$$\lambda_1 = kT / \pi P d_{12}^2, \quad (1)$$

where k is the Boltzmann constant, T is the temperature of the gas, P is the gas pressure and $d_{12} = (d_1 + d_2)/2$ is the impact parameter (d_1 and d_2 being the diameters of the species 1 and 2). Taking into account the experimental conditions and the diameter of the different species and gases, showed in Table I,²⁴ we have estimated the mean free path of the ejected atomic species Li (λ_{Li}), Nb (λ_{Nb}), and O (λ_{O}) in O₂. The results are in all cases of the order of a few mm, the mean free path of Li being approximating $\lambda_{\text{Li}} \approx 1.3$ mm. Since the ratio $\lambda_{\text{Li}}/\lambda_{\text{Nb}} \approx 1$, both species have a similar collisional probability; nevertheless $m_{\text{Li}} \ll m_{\text{Nb}}$ and thus the angular dispersion in laboratory coordinates of Li per collision is much higher than that of Nb. Consequently, the $N_{\text{Li}}/N_{\text{Nb}}$

TABLE I. Atomic (or molecular) masses and radius, taken from Ref. 23, corresponding to the different elements present in LiNbO_3 and the gases considered in this work. The estimated mean free path values in oxygen (λ) for Li, O, and Nb are also included.

Element	Mass	Radius (\AA)	λ (mm)
Li	6.94	2.05	1.3
O	16.0	0.65	3.3
Nb	92.1	2.08	1.3
He	4.00	1.09	---
O_2	32.0	1.80	---
Ar	40.0	1.82	---

ratio should decrease as the distance d to the target is increased. This reasoning agrees with the results shown in Fig. 1(b) for distances shorter than $d=33$ mm. In order to apply this reasoning to the $N_{\text{O}}/N_{\text{Nb}}$ ratio, one has to take into account the mean free path ratio ($\lambda_{\text{O}}/\lambda_{\text{Nb}} \approx 2.5$, in O_2) and the mass relationship ($m_{\text{O}} \ll m_{\text{Nb}}$). Thus, although the collision probability of O in O_2 is a 40% of that of Nb, the angular dispersion per collision is much higher for O. Therefore, it is not straightforward to predict accurately the behavior of the $N_{\text{O}}/N_{\text{Nb}}$ ratio when increasing the distance. However, since λ_{O} and σ_{Nb} in O_2 are much smaller than 33 mm, the O and Nb species will suffer several collisions before reaching the substrate. Then the $N_{\text{O}}/N_{\text{Nb}}$ ratio at this distance will be most likely dominated by the effect of the angular dispersion and therefore it should decrease, in agreement with what is observed experimentally.

The former collision-based reasoning does not explain the change of behavior observed for $N_{\text{Li}}/N_{\text{Nb}}$ and $N_{\text{O}}/N_{\text{Nb}}$ ratios for films grown at $d=40$ mm shown in Fig. 1(b). In the presence of a buffer gas and after the initial free expansion region, it has been suggested that the plasma expansion occurs in two consecutive stages:^{20,21} (i) an expansive stage in the region where the plume pressure is still higher than the gas pressure and in which the deceleration of the ejected species is observed and (ii) a diffusive stage that starts once the plume and gas pressures equilibrate, the ejected species being then transported by diffusion to the substrate. The distance at which the change of stage occurs (plume length) represents a distance related pressure threshold that has strong influence on the physical properties of the films like crystallinity,¹² refractive index,^{9,25} or roughness.²⁶ The plume length can be estimated^{20,25} within the model of adiabatic expansion as

$$L_p = A[(\gamma - 1)E]^{1/(3\gamma)} P^{-1/(3\gamma)} V^{(\gamma-1)/(\gamma-3)}, \quad (2)$$

where A is a geometrical factor related to the shape of the laser spot at the target surface, γ is the ratio of specific heats (C_p/C_v), E is the laser energy per pulse, P is the gas pressure, and V is the initial volume of the plasma ($V = v_0 \times \tau \times \text{spot size}$, v_0 being the initial species velocity, and τ the laser pulse duration). Taking into account the experimental parameters used in this work ($A=1.6$, $\tau=12$ ns and a spot size of approx. 1 mm^2) together with the expansion velocities of the ejected species measured in an earlier work⁹ ($v_0=0.8\text{--}0.9 \times 10^4$ m/s) and a value of $\gamma=1.3\text{--}1.4$,²⁰ the above formula leads to a plume length $L_p \approx 34 \pm 4$ mm. This

result suggests that at $d=20$ mm the films were grown in the expansion stage, whereas when $d=40$ mm the films were grown in the diffusion one.

As a consequence of the scattering processes which occur for distances shorter than the plume length, the angular distribution of the species at $d \approx L_p$ at which the diffusion regime starts to dominate is not the same for the different species: the lighter the species (Li and O) the broader the angular distribution. Since in the diffusion regime the species are thermalized and their movement becomes random, the species having initially the broader distribution will provide a higher relative amount of species in the forward direction, i.e., the center of the deposit in the facing substrate, as they simulate planar diffusion to a slightly higher degree. According to this reasoning, the films grown at $d=40$ mm should present an enrichment in Li and O (in respect to Nb) when compared to those grown at $d=33$ mm. This reasoning is in excellent agreement with the experimentally measured ratios shown in Fig. 1(b); therefore, it can be concluded that the composition of the films is collision or diffusion controlled for $d < L_p$ and $d > L_p$ respectively and that the Li and O content of the films is enhanced at larger distances by a diffusion controlled process. This interpretation is also in agreement with the sharp decrease in the film thickness of the films grown at $d=40$ mm [Fig. 1(a)] since for distances larger than L_p the total amount of material reaching the substrate should be significantly decreased as a consequence of the random movement of the species.

Equation (1) also indicates that the mean free path of the ejected species depends on the nature of the buffer gas and it should decrease as the radius of the gas species increases, thus increasing the collision probability. In addition, the angular dispersion per collision increases as the mass of the gas species increases. Therefore as the mass and the radius of the gas species increase, as it is our case, a larger fraction of species are deviated from their original trajectories, leading to less species reaching the substrate located in front of the target at $d=32$ mm. This reasoning is in very good agreement with the experimental results plotted in Fig. 3 which show that the thickness of the films grown on the substrate S1 (facing the target and along its normal) is lower in a gas environment than in vacuum and it decreases as the mass and radius of the gas species increases ($\text{He} \rightarrow \text{O}_2$, Ar). In order to fully understand the composition changes occurring when varying the nature of the gas (Fig. 2), the dependence of the scattering probability on the mass and radius of both the ejected and gas species has to be taken into account. Since the mean free path ratio $\lambda_{\text{Li}}/\lambda_{\text{Nb}} \approx 1$ in any of the considered atmospheres, the $N_{\text{Li}}/N_{\text{Nb}}$ ratio reaching the substrate will be mainly controlled by the mass of the gas species, and a decrease of the value of $N_{\text{Li}}/N_{\text{Nb}}$ should be expected in heavier environments in reasonably good agreement with the experimental results shown in Fig. 2.

The ratio of the oxygen to niobium mean free paths ($\lambda_{\text{O}}/\lambda_{\text{Nb}}$) decreases as the radius (and mass) of the buffer gas species increases ($\lambda_{\text{O}}/\lambda_{\text{Nb}} \approx 3.3$, 2.4 and 2.3 in He, O_2 , and Ar, respectively). Following the above reasoning, a decrease of the value of $N_{\text{O}}/N_{\text{Nb}}$ should be also observed as the mass of the gas species increases. Nevertheless, this reason-

ing is in contradiction with the experimental results shown in Fig. 2. An alternative explanation can be given by taking into account that there are be oxidized species present in the plasma which also contribute to the oxygen content in addition to atomic oxygen species.²¹ These oxidized species are heavier and they should suffer less angular dispersion than the atomic species; thus explaining why the $N_{\text{O}}/N_{\text{Nb}}$ ratio increases as the mass of the gas species increases.

The species which are preferentially scattered are the lightest species. They cannot reach the substrate located facing the target along its normal (S1) and are in part collected by the non-facing substrate S2. This interpretation is fully supported by the opposite trends of the thickness of the films grown on substrates S1 and S2 as the mass of the gas is increased (Fig. 3). The changes in film composition for those grown on the substrate S2 (either in S2GS or S2RE configuration) in the different gas environments (Fig. 4) should then be also understood in terms of scattering processes. According to the collisional framework ($\lambda_{\text{Li}}/\lambda_{\text{Nb}} \approx 1$ and $m_{\text{He}} \approx m_{\text{Li}} \ll m_{\text{Nb}}$), Nb atoms will undergo a much lower angular dispersion than Li atoms when colliding with He atoms. This fact leads to a very large $N_{\text{Li}}/N_{\text{Nb}}$ ratio in films deposited on S2 substrates in a He environment. As the mass and radius of the gas species increases (He \rightarrow O₂, Ar) the probability of suffering high angular dispersion becomes important for Nb, and then $N_{\text{Li}}/N_{\text{Nb}}$ ratio decreases in good agreement with the experimental results showed in Fig. 4. The $N_{\text{O}}/N_{\text{Nb}}$ ratio of films grown on S2 substrates in the different gas environments follows a similar trend than the $N_{\text{Li}}/N_{\text{Nb}}$ ratio. This result is not surprising since the oxygen atomic species ejected from the target are the only ones experiencing a high angular dispersion and thus contributing to the oxygen content of the films deposited onto S2 substrate. The heavier oxidized species suffer negligible dispersion.

V. CONCLUSIONS

The stoichiometric changes observed in films deposited at different target-substrate distances, in different buffer gases and substrates configuration can be understood in terms of a collisional scheme in which the lighter species are preferentially scattered by the buffer gas. The composition of the films is collision or diffusion controlled for distances shorter and longer than the plume length respectively, the relative Li content being enhanced in the diffusion regime. Finally, the preferential scattering of the lighter species leads to films enriched in Li on substrates located off the target normal.

ACKNOWLEDGMENTS

Dr. E. Diéguez (UAM, Madrid, Spain) is thanked for providing the targets, Professor R. W. Dreyfuss (I. de Optica, Madrid, Spain) is thanked for helpful discussions and comments. This work has been partially supported by CICYT (Spain) under Project TIC96-0467.

- ¹ *Properties of Lithium Niobate*, EMIS Datareviews Series, No. 5 (1989).
- ² E. Voger, in *Electro-optic and Photorefractive Materials*, edited by P. Gunter (Springer, Berlin, 1987).
- ³ C. S. Tai, Proc. IEEE **84**, 853 (1996).
- ⁴ R. A. Betts and C. W. Pitt, Electron. Lett. **21**, 960 (1985).
- ⁵ A. Yamada, H. Tamada, and M. Saitoh, Appl. Phys. Lett. **62**, 2848 (1992).
- ⁶ A. A. Wernberg, H. J. Gysling, A. J. Filo, and T. N. Blanton, Appl. Phys. Lett. **62**, 946 (1993).
- ⁷ R. C. Baumann, T. A. Roast, and T. A. Rabson, J. Appl. Phys. **68**, 2989 (1990).
- ⁸ S. B. Ogale, R. Nawathey-Dikshit, S. J. Dikshit, and S. M. Kanetkar, J. Appl. Phys. **71**, 5718 (1992).
- ⁹ C. N. Afonso, F. Vega, J. Gonzalo, and C. Zaldo, Appl. Surf. Sci. **69**, 149 (1993).
- ¹⁰ Y. Shibata, Y. Kanno, K. Kaya, M. Knai, and T. Kawai, Jpn. J. Appl. Phys. **2** **34**, L320 (1995).
- ¹¹ C. N. Afonso, J. Gonzalo, F. Vega, E. Diéguez, J. C. Cheang Wong, C. Ortega, J. Siejka, and G. Amsel, Appl. Phys. Lett. **66**, 1452 (1995).
- ¹² S.-H. Lee, T.-K. Song, T. W. Noh, and J.-H. Lee, Appl. Phys. Lett. **67**, 43 (1995).
- ¹³ K. L. Saenger, in *Pulsed Laser Deposition of Thin Films*, edited by D. B. Chrissey and G. K. Hubler (Wiley, New York, 1994), p. 582, and references therein.
- ¹⁴ C. N. Afonso, in *Materials for Optoelectronics: New Developments*, edited by F. Agulló-López (World Scientific, Singapore 1995), Chap. 1, and references therein.
- ¹⁵ N. Omori and M. Inoue, Appl. Surf. Sci. **54**, 232 (1992).
- ¹⁶ J. C. S. Kools, J. Appl. Phys. **74**, 6401 (1993).
- ¹⁷ D. B. Geohegan, in Ref. 13, p. 115.
- ¹⁸ J. Gonzalo, C. N. Afonso, and J. Perrière, Appl. Phys. Lett. **67**, 1325 (1995).
- ¹⁹ J. Gonzalo, C. N. Afonso, and I. Madariaga, J. Appl. Phys. **81**, 951 (1997).
- ²⁰ P. E. Dyer, A. Issa, and P. H. Key, Appl. Surf. Sci. **46**, 89 (1990).
- ²¹ W. K. A. Kummuduni, Y. Nakayama, Y. Nakata, T. Okada, and M. Maeda, J. Appl. Phys. **74**, 7510 (1993).
- ²² H. S. Kwok, Appl. Surf. Sci. **109/110**, 595 (1997).
- ²³ S. Dushman, *Scientific Foundations of Vacuum Technique* (Wiley, New York, 1962), Chap. 1.
- ²⁴ Periodic Table of Elements (SMI Corp., 1991); R. A. Alberty and R. J. Silbey, *Physical Chemistry* (Wiley, New York, 1992), Chap. 18.
- ²⁵ J. Gonzalo, C. N. Afonso, and J. M. Ballesteros, Appl. Surf. Sci. **109/110**, 606 (1997).
- ²⁶ I. Zhang, D. Cui, Y. Zhou, L. Li, Z. Chen, M. Sazbadi, and P. Hess, Thin Solid Films **287**, 101 (1996).